Acta Cryst. (1961). **14**, 11

Electron Diffraction Studies on Solid α-Nitrogen*

By Erwin M. Hörl and L. Marton

National Bureau of Standards, Washington, D.C., U.S.A.

(*Received* 6 *February* 1960)

A technique was developed for studying thin films of solidified permanent gases by means of electron transmission diffraction. It was applied to the investigation of thin films of solid α-nitrogen at 4 and 20 °K. The orientation of the microcrystallites on aluminum and Formvar substrates was investigated as a function of both the temperature of the substrate and the intensity of the molecular nitrogen beam during deposition. Further, the crystal structure and the cell dimensions of α-nitrogen were reinvestigated. Faults in the stacking sequence of (111) planes, detected under certain conditions, were studied in some detail. Preferential crystal growth processes were observed to be induced by electron bombardment. The influence of conditions of deposition on these processes was also investigated.

Introduction

There has been considerable research in recent years on the emission of light from nitrogen atoms and other radicals stabilized in α-N_2 matrices at very low temperatures (Bass & Broida, 1956; Herzfeld & Broida, 1956; Broida & Peyron, 1957; Herzfeld, 1957; Broida & Peyron, 1958; Peyron & Broida, 1959; Hörl, 1959; Peyron, Hörl, Brown & Broida, 1959). This work stimulated interest in the detailed investigation of the structure of thin films of α-nitrogen produced by condensation of nitrogen gas on cold surfaces.

The most interesting questions to be answered were: Are the thin films obtained by condensation of gaseous nitrogen on cold surfaces amorphous or crystalline? If crystalline, do the crystals exhibit a preferred orientation, and what is their averages size? Are there stacking faults and strain systems present? In what way are these phenomena dependent upon the type and temperature of the substrate, and how are they affected by the conditions of gas flow during the condensation process?

Further, it was desirable to settle existing disagreement on the structure of α-nitrogen, the modification which is stable below 35·5 °K. Vegard (1929) proposed the T^4-space group, while Ruheman (1932) suggested the T_h^6-space group. A recent X-ray re-examination (Bolz *et al.*, 1959) of solid nitrogen eliminated Vegard's arguments for T^4 and thus made T_h^6 very probable. In the Ruhemann structure, the arrangement of the molecule centers is exactly face-centered cubic; in the Vegard structure, they are shifted slightly from face-centered cubic positions.

Experimental technique

The cryostat used in our experiments has been described in detail in an earlier publication (Hörl & Marton, 1958). A simplified vertical cross section of its lower part is presented in Fig. 1. Mounted on the copper target block is a thin Al or Formvar foil upon which the nitrogen gas is condensed. Good heat contact is maintained between the target block and the cooling bath (liquid helium or liquid hydrogen). The temperature of the target block can be measured by means of a carbon resistance thermometer. An electron beam of 46 kV. passes through the foil and solidified gas layer either perpendicularly or at smaller angles of incidence. The transmission diffraction pattern can be observed visually or photographed.

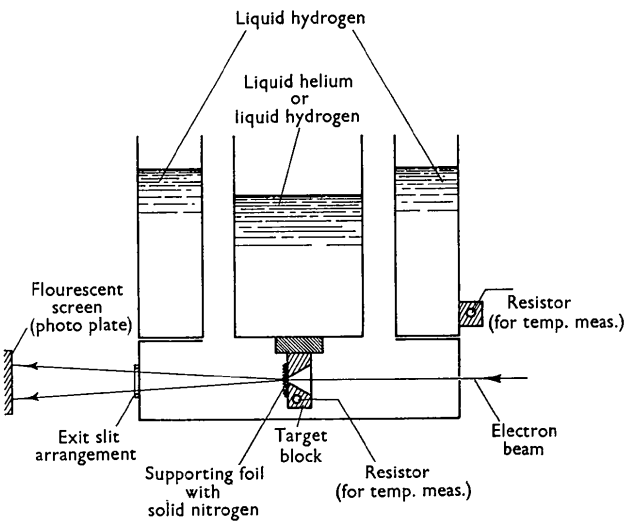

Fig. 1. Simplified vertical cross section of the lower part of the cryostat, showing the arrangement of target, radiation shield, and cooling baths.

In extending electron diffraction technique to solidified permanent gases, we were faced with two major experimental difficulties: first, condensation of the residual gases of the high vacuum system on the cold

* This research was performed under the National Bureau of Standards Free Radicals Research Program, supported by the Department of the Army.

target surface; and, second, electrical charging effects due to the high electrical resistance of solid nitrogen. The condensation problem was reduced below the observable limit by the reduction of background pressure in the outside parts of the system to 1×10^{-7} mm. Hg. This was achieved through the use of liquid hydrogen rather than liquid nitrogen for cooling the radiation shield. In addition, the sizes of the openings in the radiation shield were reduced to a minimum. The charging effects were due to the thin N_2 film condensed on the whole target block area and on the inner walls of the radiation shield. Condensation occurred over the entire inner surface because the sticking coefficients of N_2 gas on surfaces at temperatures 4 and 20 °K. are less than 1 (Foner *et al.*, 1959). Two techniques were employed to prevent charging effects: first, the electron beam was made very fine and narrow in order to reduce the number of stray electrons which could produce charging; and, secondly, a modification of the inner surface was introduced where the diffracted beam hits. This was done by using a 'temperature floating' exit slit as shown in Fig. 2. A thin, thermally insulated Al foil was mounted on the radiation shield, so that it received radiation on one side from room temperature surfaces and on the other side from 20 °K. and 4 °K. surfaces. Thus it stayed warm enough to prevent condensation of nitrogen upon itself. A slit was used in preference to a round aperture to satisfy the minimum opening requirement in the radiation shield together with the requirement of recording electrons diffracted at large angles.

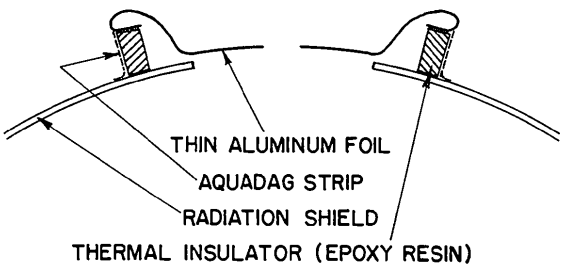

Fig. 2. 'Temperature floating' exit slit (horizontal cross section ⊥ slit).

Our work was done primarily at 4 and 20 °K., with liquid helium or liquid hydrogen as a cooling bath. In some experiments, the film structure was also observed during warm-up.

The combined thickness of the supporting foil and the condensed nitrogen layer was kept so small that, for the most part, an electron underwent only one scattering event. Thus, the observed electron diffraction patterns were simple superpositions of the pattern which would have been observed for the supporting foil or the condensate alone.

In most experiments we used polycrystalline Al or Formvar substrates 200–300 Å thick. To observe N_2 diffraction rings masked by Al rings, we used in some experiments Al foil with orientation of the microcrystallites [(111) || foil plane]. The polycrystalline Al foils were prepared by evaporation of Al in vacuum on a glass surface which was pre-coated with NaCl. The highly oriented Al foils were produced by epitaxy on rock salt. In both cases, the foils were floated off on a water surface and mounted. The Formvar substrates were prepared by dropping a few drops of a 0·5% solution of Formvar in ethylene dichloride on a water surface.

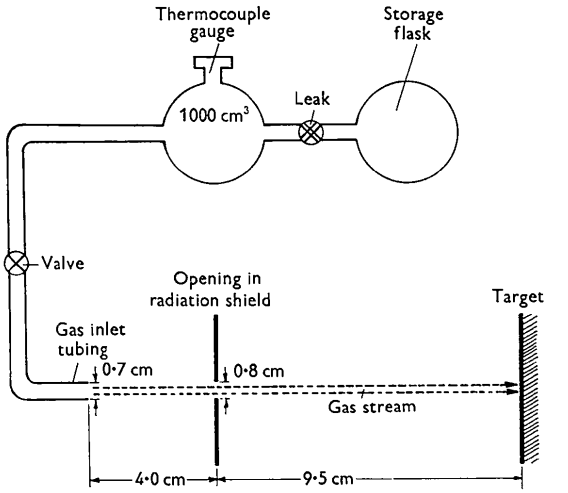

Fig. 3. Gas inlet system (schematically).

The nitrogen gas was admitted by means of a flow system shown schematically in Fig. 3. It operated in the following way: first, the 1000 cm.³ glass flask was filled with nitrogen gas to a pressure of a few hundred microns Hg. Then, the valves were opened and manually regulated to keep the rate of pressure decrease in the flask at a pre-determined constant value. In this way, the flow rate and the total amount of gas introduced into the system was known and could be preset.

Throughout this paper we shall refer to low, medium, and high flow rates. They correspond to the following numbers: 0·001 cm.³(s.t.p.)/sec., 0·005 cm.³(s.t.p.)/sec., and 0·03 cm.³(s.t.p.)/sec. These flow rates cover the range which could be easily handled using the above-described technique.

Estimates of thickness and build-up speed (layers/sec.) of the nitrogen condensates were made from the geometry of the gas inlet system and the measured rate of gas flow.* A sticking coefficient of 0·6 was

* Mayer (1929) has shown that

$$\left(\frac{dN}{N}\right)_{\substack{\text{opening in thin wall}\\ \text{(cosine distribution)}}} = \frac{1}{5{\cdot}5}\left(\frac{dN}{N}\right)_{\substack{\text{channel (length} \gtrapprox\\ 2 \times \text{diameter)}}}$$

where dN is the number of molecules leaving the source per time unit in the forward direction in a small space angle $d\omega$, and N the total number of molecules leaving the source per time unit. The necessary condition for molecular flow—collision-free path length of molecules in source chamber

assumed for the gas molecules on the cold target surface (Foner *et al.*, 1959). Under these assumptions and conditions, the estimated build-up speeds were: 0·2 layers/sec. for the low flow rate case, 1 layer/sec., and 6 layers/sec. for the medium and high flow rate cases. Completely independent estimates, using the different atomic scattering factors for electrons for N_2 and Al, gave figures of the same order of magnitude. The film thicknesses were estimated by the product of build-up speed and total deposition time. They were in most of our experiments of the order of a few hundred Ångströms.

In order to measure the lattice parameters of α-nitrogen, we used the diffraction pattern of the Al substrate as a standard. The lattice parameter of Al has been measured with high precision by means of X-rays at temperatures as low as 20 °K. (Figgins *et al.*, 1956). There was some doubt as to the validity of the assumption that our thin films evaporated in vacuum from a tantalum crucible have the same lattice constant as was given by the X-ray measurements. It is known that in evaporation from a tungsten crucible the formation of an alloy occurs, reducing the lattice parameter considerably (*Encyclopedia of Physics*, 1957). We could find no information on the alloy-forming effect of tantalum crucibles; consequently, we checked the lattice constant a_{Al} of these Al foils using MgO which gives a very sharp (200) diffraction ring. MgO was deposited on the Al foils and from the two superimposed patterns a_{Al} was calculated. The value $a_0 = 4{\cdot}213$ Å (Swanson & Tatge, *National Bureau of Standards Circular* 539, Vol. 1) was used for the lattice constant of MgO. The check revealed no significant deviation from the well-known lattice constant of aluminum (Figgins *et al.*, 1956).

The nitrogen gas used in these experiments, according to the commercial supplier, had as main impurities < 10 p.p.m. of oxygen and about 50 p.p.m. of argon.

(oven) $\gtrapprox 2 \times$ diameter of gas inlet tubing—was tested experimentally by measuring the gas pressure at the beginning of the 18 cm. long gas inlet tube. The pressure amounted to 3, 12, and 70 microns Hg in the low, medium, and high flow rate cases, respectively, and fulfilled the requirements, certainly in the low flow rate case.

EXPERIMENTAL RESULTS AND INTERPRETATION

Structures of α-nitrogen films

(*a*) *Nitrogen deposits on aluminum substrates at* 4 °K.

At slow flow rates (corresponding to build-up speeds $\approx 0{\cdot}2$ layers/sec.) diffraction patterns of the condensate showed one broad, diffuse diffraction ring at the position where the 111 and 200 reflections are expected to occur (Fig. 4). Increasing the thickness of the condensed nitrogen layer did not change the structure of this ring. Further, diffraction patterns taken at angles of incidence of 50° did not differ from those taken at 90° (beam $\perp$ foil). In particular, no change in intensity along the diffraction ring could be observed in the 50° cases.

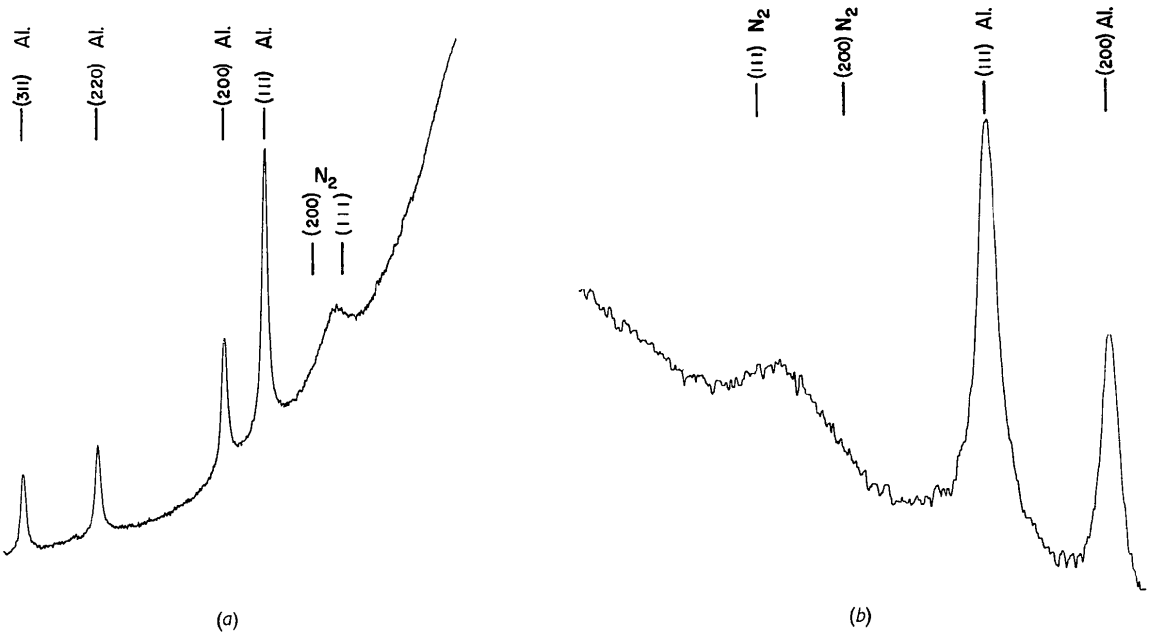

Fig. 4. Plate transmission tracings of a diffraction pattern of a thin film of solid α-nitrogen obtained by condensation of nitrogen gas on an Al substrate at 4 °K. at a flow rate corresponding to a layer build-up speed of $\approx 0{\cdot}2$ layers/sec. (slow flow rate). Electron beam $\perp$ substrate. The α-nitrogen reflections indicated by marks correspond to large ideal crystals. (*a*) Complete tracing of plate showing pattern of the Al substrate with superimposed nitrogen pattern (diffuse ring). (*b*) Detail tracing of diffuse nitrogen ring, taken at slow densitometer speed, showing the exact line profile.

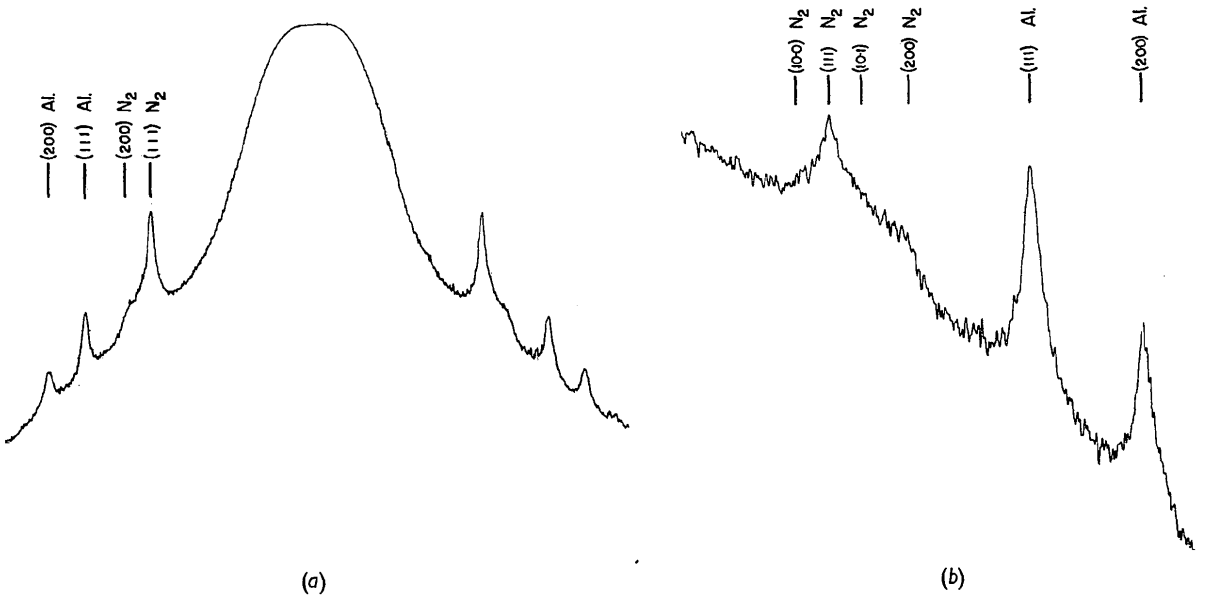

Fig. 5. Plate transmission tracings of diffraction patterns of thin films of solid α-nitrogen obtained by condensation of nitrogen gas on Al substrates at 4 °K. at a flow rate corresponding to a layer build-up speed of ≈ 1 layer/sec. (medium flow rate case). Electron beam ⊥ foil. The α-nitrogen reflections indicated by vertical lines correspond to large ideal crystals. (*a*) Plate tracing showing complete pattern of Al substrate and α-nitrogen condensate. (*b*) Tracing of 111...200 region of α-nitrogen (deposited layer considerably thinner than in Fig. 5(*a*)).

These diffraction patterns indicate that the condensed layer was amorphous. A Fourier analysis of these patterns is presently being carried out.

The use of medium flow rates (corresponding to build-up speeds ≈ 1 layer/sec.) in the deposition process results in a diffraction pattern of which the intensity profile of the 111...200 region is as shown in Fig. 5. The 111 reflection is sharp, but differs from the line profile of ideal crystals by a strong broadening of the line base (compare 111 α-N_2 with 111 Al). The 200 reflection is broad and diffuse and on some plates not distinctly separated from 111. It was, in all cases, lower in area intensity than would be expected from ideally built crystals. Also on some plates a very faint trace of the hexagonal 10·0 reflection is visible. Higher order reflections were immeasurable due to masking or lack of intensity.

Patterns taken at angles of incidence of 50° and 40° did not show noticeable differences in the intensity profile of the 111...200 region in comparison with patterns made at 90° (beam ⊥ foil). Further, no changes in intensity along the rings could be observed in any of the patterns.

The observed diffraction patterns can be interpreted by random crystal orientation in the condensed layer and by faults in the stacking of the (111) planes of the individual microcrystallites. No tensile strain seems to be present (no change in line profile when target is turned in respect to electron beam). The size of the crystals determined by the half-width of the 111 reflection was 50–300 Å. The stacking faults will be discussed in detail later.

High flow rates (corresponding to build-up speeds ≈ 6 layers/sec.) resulted in a diffraction pattern very similar to the one described for medium flow rates. Again patterns were taken at angles of incidence of 45° and 90°, and the result was the same as for the medium flow rate case. It is remarkable that the film structure of a very thin deposit was very much like that described for slow flow rates.

The experiments, especially the ones in which low flow rates were used, were performed with short 'beam-on' periods. A slow recrystallization process was observed when the electron beam was left on continuously, indicating that the heat input into the deposit by the electron beam was not negligible. The diffraction pattern described for the slow flow rate case was changed to one characteristic of medium flow rates in a 'beam-on' period of 20 min. After 10 min. a faint (111) ring was visible. Long 'beam-on' periods caused a sharpening of the (200) ring in the medium flow rate pattern.

(*b*) *Nitrogen deposits on Formvar substrates at* 4 °K.

Diffraction patterns on Formvar were very similar to the ones observed with Al substrates. The main difference was the very strong recrystallization effect of the electron beam on the condensate due to the low thermal conductivity of Formvar as compared to the metal Al. In only one to three min. 'beam-on' period, a deposit characteristic of slow flow rates (broad, diffuse diffraction ring) was changed to a pattern characteristic of medium flow rates (Fig. 6).

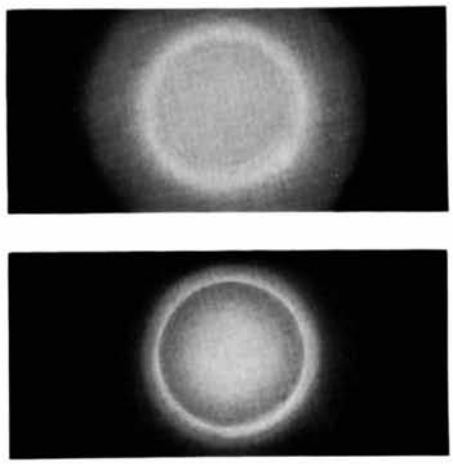

Fig. 6. Recrystallization process due to heating of target by the electron beam. Nitrogen gas had been condensed on a Formvar foil at 4 °K. In order to observe the structure change of the deposit with time during electron irradiation, the electron beam was transmitted through the foil for two minutes. Electron beam ⊥ foil. (*a*) Diffraction pattern immediately after the beam was turned on. (*b*) Diffraction pattern after 2 minutes 'beam on' period.

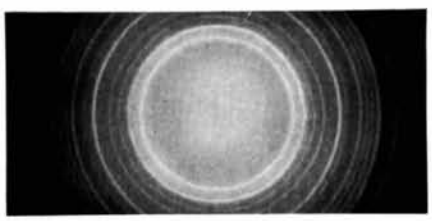

Fig. 8. Electron diffraction pattern obtained from a α-nitrogen layer on a Formvar substrate at 20 °K. Angle of incidence of electron beam with respect to foil was 45°. No change of intensity along the diffraction rings could be detected.

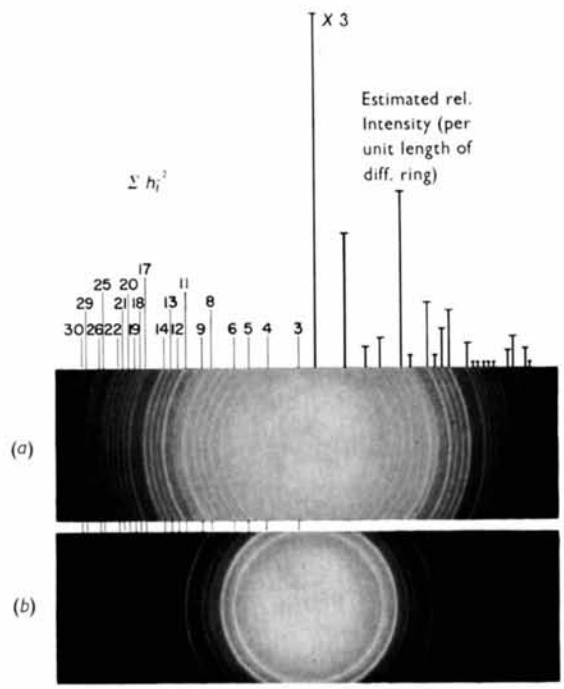

Fig. 7. Electron diffraction pattern obtained from a α-nitrogen layer on a Formvar substrate at 20 °K. Electron beam ⊥ foil. (*a*) Long exposure to make higher order reflections visible. (*b*) Short exposure to obtain distinct pattern of low order reflections.

[*To face p.* 14

(c) *Nitrogen deposits on aluminum and Formvar substrates at* 20 °K.

Neither flow rate nor substrate type detectably influenced the condensate structure when nitrogen gas was condensed on Al or Formvar at 20 °K. In every experiment at this temperature, sharp line patterns were obtained (Fig. 7). Again, patterns were taken at angles of beam incidence of 45° and 90° and no change of intensity along the diffraction rings could be observed (Fig. 8).

From the line width, an average crystal size of a few hundred Å could be calculated, which is of the same order of magnitude as the layer thickness. As indicated above, no azimuthal change of intensity could be detected in the patterns taken at inclined beam incidence; one must conclude, therefore, that no preferential crystal orientation took place. From the relative intensities of the reflections and their spacings, information on crystal structure and lattice parameter could be obtained. This will be discussed later.

(d) *Change of nitrogen film structure during warm-up*

Deposits obtained by condensing nitrogen gas on Al substrates at 4 °K. changed their structures gradually during warm-up, becoming more and more similar to deposits obtained by condensing nitrogen gas on 20 °K. substrates. This indicated a recrystallizing and annealing process, as one would expect. The deposits migrated or evaporated off the substrate at temperatures around 26 °K. In no case could we observe a nitrogen pattern at 30 °K. For this reason, it was not possible to observe the phase transition from α to β nitrogen, which takes place at 35·5 °K.

Crystal structure and cell dimensions

The first structure determination of solid α-nitrogen was made by Vegard (1929). He used the X-ray powder method and found as a result a molecular lattice of the $T^4(P2_13)$ space group. The centers of the nitrogen molecules were arranged in such a way that they were shifted slightly from face-centered cubic positions. The internuclear distance of the two nitrogen atoms of the nitrogen molecule was determined to be 1·065 Å, a value very close to or identical with the value for the free gas molecule.

This somewhat peculiar result was checked in 1932 by Ruhemann using the same technique as Vegard. Ruhemann found that the $T_h^6(Pa3)$ space group may also be regarded as a possible one. He pointed out that the 110 reflection, which is necessary for Vegard's structure and which was observed by Vegard, may have been a $K\beta$ reflection. In the T_h^6 space group, the arrangement of the molecule centers is exactly face-centered cubic and the coordinates of the atoms comprising the four molecules of the cubic elementary cell are:

$$[(p, p, p),\ (-p, -p, -p)],$$
$$[(\tfrac{1}{2}-p, -p, \tfrac{1}{2}+p),\ (\tfrac{1}{2}+p, p, \tfrac{1}{2}-p)],$$
$$[(\tfrac{1}{2}-p, \tfrac{1}{2}+p, p),\ (\tfrac{1}{2}+p, \tfrac{1}{2}-p, -p)],$$
$$\text{and } [(-p, \tfrac{1}{2}+p, \tfrac{1}{2}-p),\ (p, \tfrac{1}{2}-p, \tfrac{1}{2}+p)].$$

A picture of a model of this unit cell is shown in Fig. 9.

The lattice parameter as measured by Vegard (1929) at 20 °K. was 5·66 Å; Ruhemann's (1932) value was $5{\cdot}67 \pm 0{\cdot}02$ Å. A value for 4 °K. of $5{\cdot}644 \pm 0{\cdot}005$ Å was given by Bolz *et al.* (1959). Our measurements on plates from several different runs at 20 °K. agreed within the error of measurement and gave $a_{20\,^\circ\mathrm{K}} = 5{\cdot}661 \pm 0{\cdot}008$ Å.

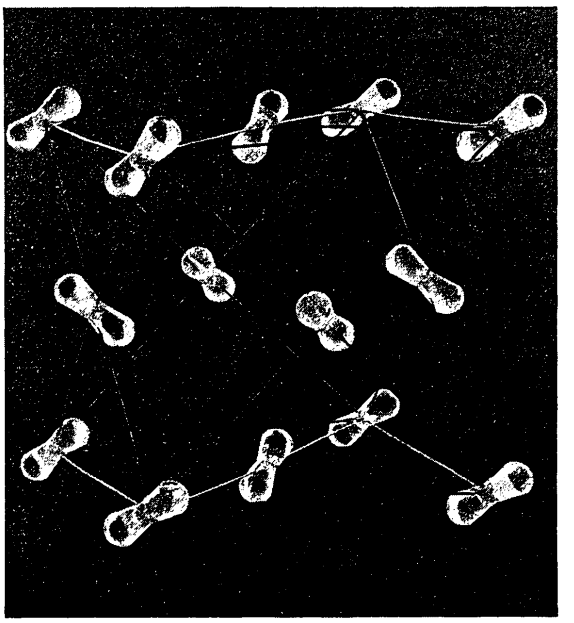

Fig. 9. Model of cubic unit cell of the α-nitrogen lattice according to the Ruhemann structure.

Our visual estimates of the intensities of the observed electron diffraction rings of nitrogen condensates at 20 °K. on Formvar foils agree well with the Ruhemann structure with the exception of the 200 reflection. This discrepancy is most probably due to some stacking faults still present in 20 °K.-deposits. In Table 1, visual estimates of the intensities of our diffraction rings are compared with relative intensities calculated on the basis of the Ruhemann structure, assuming an internuclear distance of the atoms of each molecule identical with the gas phase value (1·094 Å; Herzberg, 1955) and a lattice parameter of 5·661 Å. From this agreement, one can conclude that the internuclear distance of the atoms of each nitrogen molecule in the α-solid is close to the gas phase value. A $\pm 20\%$ deviation of the internuclear distance from the gas phase value would have shown very distinct differences even in visual estimates of the diffraction ring intensities.

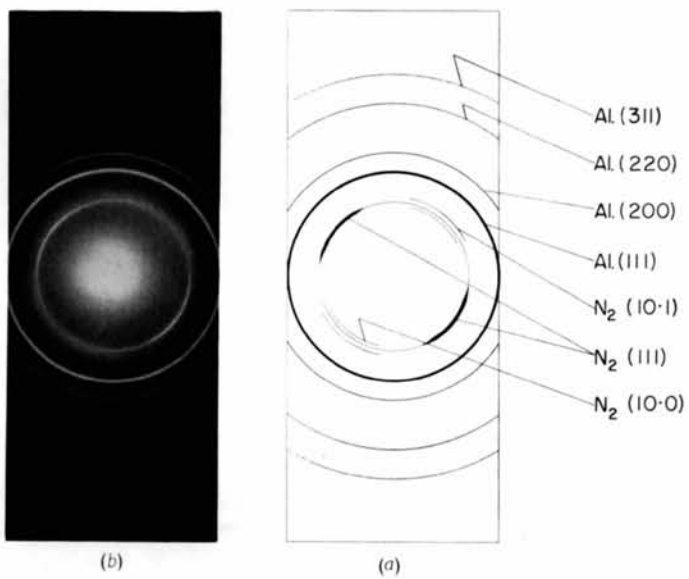

Fig. 12. Electron transmission diffraction pattern obtained after electron bombardment treatment from a polycrystalline nitrogen film of originally random crystal orientation.

Table 1. *Relative intensities of α-nitrogen diffraction rings*

Σh_i^2	Group of reflecting planes	Relative experimental intensities: Vegard (1929)	Ruhemann (1932)	Present paper*	Relative theoretical intensities of Ruhemann structure†
1	(100)	—	—	0	0
2	(110)	20	—	0	0
3	(111)	150	*sst*	12000	13700
4	(200)	100	*st*	1500	5260
5	(210)	20	*s*	250	578
6	(211)	25	*ms*	350	715
8	(220)	75	*mst*	2000	1530
9	(300)	20	*ss*	150	0
	(221)				201
10	(310)	3	—	0	0
11	(311)	60	*m*	700	861
12	(222)	15	*ss*	150	242
13	(320)	30	*s*	400	472
14	(321)	50	*m*	600	730
16	(400)	2	—	0	12·8
17	(322)	30	*ms*	250	290
18	(411)	15	*ms*	50	138
19	(331)	15	*ss*	50	64·3
20	(420)	5	—	50	17·5
21	(421)	5	—	50	63·2
22	(332)	15	—	50	64·5
24	(422)	10	—	0	7·1
25	(500)	35	—	200	0
	(430)				216
26	(431)	50	*ss*	350	360
	(510)				0
27	(333)	—	—	0	2·5
	(511)	—	—		12·4
29	(520)	660	—	200	81·6
	(432)				176
30	(521)	40	—	50	131

sst—very strong; *st*—strong; *mst*—medium strong; *m*—medium; *s*—weak; *ms*—medium weak; *ss*—very weak.

* Visual estimates taken from a diffraction pattern of a nitrogen condensate on a Formvar substrate at 20 °K. (Intensities per unit length of diffraction ring).

† The theoretical intensity for a cubic structure per unit length of diffraction ring for the reflection group $\Sigma h_i^2 = \text{const.}$ is given by:

$$I_{\Sigma h_i^2} = \text{const.}\,[(Z-F_r)^2/(\Sigma h_i^2)^3]\,\Sigma\Big(\sum_k \exp\,(2\pi i/a).(x_k h_1 + y_k h_2 + z_k h_3)\Big)^2,$$

where Z is the nuclear charge, F_r the atomic X-ray scattering factor, a the lattice constant, x_k, y_k, and z_k the subcoordinates for the atoms of one cell.

Structure imperfections

Fig. 5 shows the plate transmission tracings of electron diffraction patterns obtained from nitrogen films prepared by deposition of nitrogen gas on Al foils at 4 °K., with medium flow rate. The main anomalies of the observed intensity profile of the 111...200 region lie in the reduced intensity and broadening of the 200 reflection, the broadening of the line base of the 111 reflection, and the appearance of a very faint trace of a 10·0 reflection on some plates. These phenomena strongly suggest interpretation in terms of stacking faults of the (111) planes.

(*a*) *Stacking faults of the first kind*

The arrangement of the molecule centers in the α-nitrogen lattice is of the face-centered cubic type. Thus we can build the crystal by stacking A, B, and C type (111) layers: $\ldots ABCABCABC\ldots$, as shown in Fig. 10. However, this sequence may be disturbed by growth faults: $\ldots ABCA\bar{B}(A)CBA\ldots$ when (A) is the faulted plane.† In this case, the structure is symmetrical with respect to one of the planes (marked in the example above by a bar); therefore, this type of irregularity in the stacking sequence is referred to as 'twin faulting'. We assume all the A-, B-, or C-type planes, respectively, to be completely identical in all X and Y coordinates (X and $Y \parallel (111)$) of corresponding atoms. This type of fault we shall call a stacking fault of the first kind.

(*b*) *Stacking faults of the second kind*

A second type of fault in the stacking of the (111) planes of α-nitrogen is predicted by the fact that the symmetry of the T_h^6 space group is lower than that of

† The analogous sequence for a deformation fault would be: $\ldots ABCAB(A)BCA\ldots$.

the O_h^5 space group of a simple face-centered cubic structure. This second fault type is characterized by the fact that the molecule centers are not affected. In Fig. 10, one can distinguish 4 types of N_2 molecules in (111) planes according to their angular position in space. These four types are designated *P*-, *Q*-, *R*-, and *S*-types molecules; the shortest distance between two molecule centers in the (111) plane we shall call a^*.

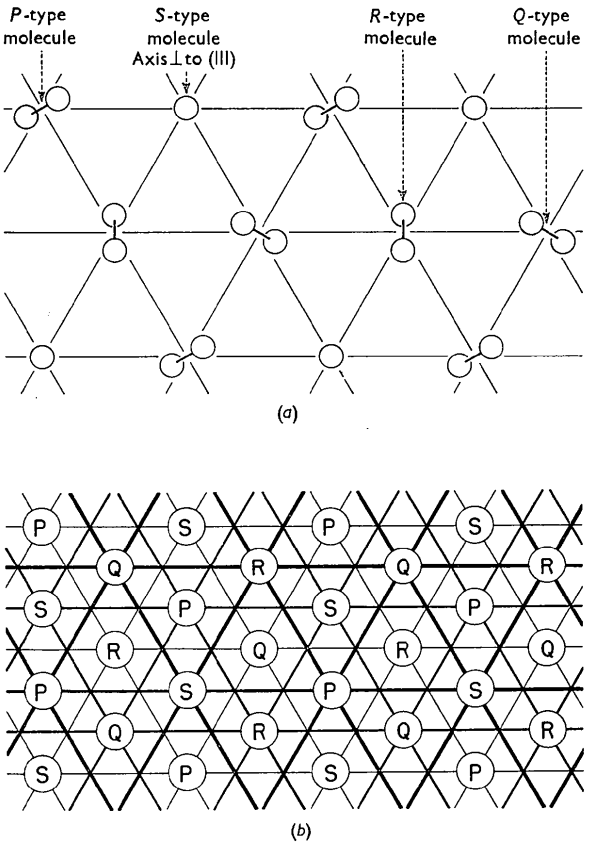

Fig. 10. (*a*) Single (111) plane of the α-nitrogen crystal lattice. One can distinguish 4 types of N_2 molecules according to their positions in space (*P*, *Q*, *R*, and *S*). (*b*) The α-nitrogen crystal lattice built up by the stacking of *A*-, *B*-, and *C*-type (111) planes. The different types of planes are distinguished by the different widths of the connecting lines.

It is obvious that we can now introduce faults in the stacking sequence of the ideal crystal lattice by shifting a given (111) plane, and all the following (111) planes by a distance of a^* along a [10·0] or [01·0] or [11·0] direction, making parallel molecule pairs in adjacent layers nearest neighbors. Furthermore, the arrangement of *P*-, *Q*-, *R*- and *S*-type molecules in a (111) net plane can be changed, yielding an infinite number of possible stacking faults of the second kind.

(*c*) *Effects of stacking faults on the electron diffraction pattern*

A considerable amount of experimental and theoretical work has been done in the last twenty years on faults in the stacking sequences of crystal planes (Edwards & Lipson, 1942; Wilson, 1942; Paterson, 1952; Kimoto, 1953; Hosemann & Bagchi, 1954). A number of similar theoretical approaches have been used, but only the close-packed hexagonal or face-centered cubic structure could be treated under the assumption of uniform fault distribution.

Therefore we are forced to treat the α-nitrogen crystal structure as a simple f.c.c. structure. Stacking faults of the second kind therefore must be neglected, and the molecules considered as single scattering centers. This approximation seems justifiable for the low order reflections (111, 200 and 220), for which the interplanar distance is large in comparison with one-half the internuclear distance of the N_2 molecule. These reflections are very strong in comparison with the 210 and 211 reflections (see Table 1); the intensity relationships 111:200:220 resemble those predicted for the simple f.c.c. structure.

We must further assume a completely uniform fault distribution in the real α-nitrogen crystallites in order to apply the theory. Very faint traces of 10·0 reflections were visible on some plates, indicating the existence of regions with a fault probability, α, in the range $\frac{1}{2} < \alpha < 1$. However, the main anomalies of the pattern (Fig. 5) are characteristic of an α in the range $0 < \alpha < 2/3 - 3$ (Paterson, 1952). This indicates some clustering of faults in the real crystals. The theoretical expressions for intensity distribution in the reciprocal lattice are no longer strictly applicable, but can still give a qualitative picture of the situation in the real crystallites.

The anomalous appearance of the 200 reflection is characteristic of stacking faults in (111) planes of f.c.c. crystals with α in the range $0 < \alpha < 2/3 - 3$ (Paterson, 1952). According to the formulas in Appendix II of Paterson (1952), a shift of the maximum of the 200 reflection toward the 111 peak should occur. The amount of this shift for $\alpha = 0{\cdot}1$ was calculated to be 0·03% of the ring radius of 200, for an $\alpha = 0{\cdot}2$ to be 0·15%. Because of the diffuseness of the 200 reflection, such a shift is difficult to detect. On none of our plates was such a shift clearly visible.

The most probable reason for the broadening of the line base of the 111 reflection is the appearance of diffuse hexagonal 10·0 and 10·1 reflections due to highly faulted regions ($\frac{1}{2} < \alpha < 1$).

In interpreting the observed pattern, one must also consider that a certain amount of very fine crystalline powder may be present together with faulted crystals of larger size; an exact line intensity profile analysis, therefore, is very difficult or even impossible to perform.

Preferred crystal growth

Experiments were performed in which nitrogen gas was deposited on a 4 °K. aluminum target at medium flow rates, and bombarded with a 46 kV., 3 to 30 μA.

electron beam of a few millimeters diameter as shown in Fig. 11. Electrons impinged on the target block at a small angle, 5° to 15°, striking only the area below the 0·1 mm. aperture at the beginning of the bombardment procedure. The beam was then moved upward over the target at a slow speed of ≈ 1 mm./sec. and cut off after it had passed the specimen.

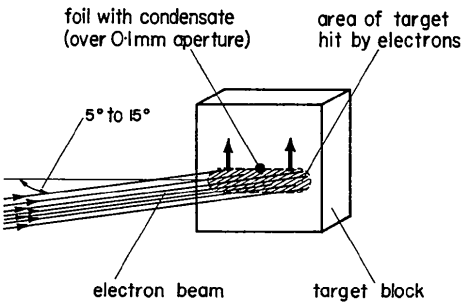

Fig. 11. Procedure for electron bombardment treatment for preferred crystal growth.

The transmission diffraction pattern (electron beam ⊥ foil) obtained after this bombardment treatment is shown in Fig. 12*. A very distinct variation in intensity appears along the (111) diffraction ring. Further, the hexagonal 10·0 and 10·1 reflections of β-nitrogen appear along the weak intensity parts of (111). The (222) diffraction ring, not shown in the figure, shows the same intensity distribution as the (111) ring. Weaker sections of the (311) ring occur at the same azimuthal angle as the maxima of the (111) and (222). All other reflections of the nitrogen film are either too weak for a clear detection of intensity changes, or masked by aluminum reflections.

The straight line connecting the intensity maxima of the (111) ring was never exactly perpendicular nor parallel to the direction of the upward motion of the bombarding beam, but it was always much more nearly perpendicular than parallel.

When the specimen was rotated around an axis perpendicular to the electron beam, the intensity maxima of the (111) ring decreased; the minima increased. At an angle of 25° from the original position (beam ⊥ foil) this effect was quite pronounced, and at 40° a completely uniform (111) ring was observed. Rotation of the target thus permitted observation of the distribution of [111] directions of the microcrystallites over a large space angle. On a unit sphere the [111] density distribution shows two approximately circular areas of high density opposite each other. The line connecting the centers of these areas is nearly perpendicular to the upward motion of the bombarding beam and also perpendicular to the line connecting the target foil with the center of the photographic plate.

No orientation of the microcrystallites could be obtained with the above-described technique when nitrogen gas was condensed on a 20 °K. substrate and bombarded at the same temperature. A sample prepared by condensation on a 20 °K. substrate was bombarded at 4 °K. Again, no orientation could be obtained.

These observations suggest a preferred crystal growth process during the bombardment caused, perhaps, by a thermal gradient built up at the border line between the irradiated and unirradiated parts of the target surface. Apparently the gradient moves over the area of the target hole when the beam moves upward. Under this thermal treatment, crystals grow in such a way that the [111] direction is, within a certain range, parallel to the supporting foil and perpendicular to the gradient. The intensity maxima of the (111) diffraction ring should be on a line exactly perpendicular to the direction of motion of the bombarding beam (this is also the expected direction of the thermal gradient). In practice, however, it is probably impossible to control the movement of the thermal gradient over the very small area of the target hole so precisely, even with an exactly horizontal beam. Therefore, the connecting line between the (111) maxima can not be expected to be exactly horizontal.

The intensity variation along the 311 reflection seems to indicate random azimuthal arrangement of the crystallites with respect to the [111] direction; no particular crystal plane seems to be parallel to the substrate.

Hexagonal reflections appear, probably as a result of the heating of some part of the nitrogen deposit during bombardment to a temperature above 35 °K. Hexagonal crystals may be formed in this process and may grow with their [00·1] directions perpendicular to the thermal gradient. Since a quenching of the hexagonal β-modification may be possible in a somewhat disordered structure, the (10·0) and (10·1) planes of the hexagonal crystals could reflect, after bombardment, when the diffraction pattern is observed. A second interpretation of the appearance of hexagonal reflections may be based upon the assumption of the existence of highly faulted regions between ideally grown, larger crystals; however, the orientation of the crystallites would be difficult to understand.

Preferred crystal growth is induced by electron bombardment only if the microcrystallites are strongly faulted (stacking faults of the (111) planes). Deposits condensed at 20 °K., which are nearly fault-free, exhibited no orientation phenomena under bombardment. These observations may be understood from current theories on the recrystallization process (Schmid & Boas, 1935).

The authors wish to thank Miss LaBonnie A. Bianchi for very excellent assistance throughout the work, Mr Jimmie A. Suddeth for taking diffraction patterns of Al substrates for calibration, and Mr Mardell D. Wagner for preparing excellent drawings.

* Plate 2.

References

BASS, A. M. & BROIDA, H. P. (1956). *Phys. Rev.* **101**, 1740.

BOLZ, L. H., BOYD, M. E., MAUER, F. A. & PEISER, H. S. (1959). *Acta Cryst.* **12**, 247.

BROIDA, H. P. & PEYRON, M. (1957). *J. Phys. Radium*, **18**, 593.

BROIDA, H. P. & PEYRON, M. (1958). *J. Phys. Radium*, **19**, 480.

EDWARDS, O. S. & LIPSON, H. (1942). *Proc. Roy. Soc.* A, **180**, 268.

Encyclopedia of Physics (1957). XXXII, 451. Edited by S. FLÜGGE.

FIGGINS, B. F., JONES, G. O. & RILEY, D. P. (1956). *Phil. Mag.* 8/1, 747.

FONER, S. N., MAUER, F. A. & BOLZ, L. H. (1959). (The National Bureau of Standards, Washington, D.C.) Private communication.

HERZBERG, G. (1955). *Spectra of Diatomic Molecules*, London.

HERZFELD, C. M. & BROIDA, H. P. (1956). *Phys. Rev.* **101**, 606.

HERZFELD, C. M. (1957). *Phys. Rev.* **107**, 1239.

HOSEMANN, R. & BAGCHI, S. N. (1954). *Phys. Rev.* **94**, 71.

HÖRL, E. M. & MARTON, L. (1958). *Rev. Sci. Instrum.* **29**, 859.

HÖRL, E. M. (1959). *J. Mol. Spec.* **3**, 425.

KIMOTO, K. (1953). *J. Phys. Soc. Jap.* **8**, 762.

MAYER, H. (1929). *Z. Phys.* **58**, 373.

PATERSON, M. S. (1952). *J. Appl. Phys.* **23**, 805.

PEYRON, M. & BROIDA, H. P. (1959). *J. Chem. Phys.* **30**, 139.

PEYRON, M., HÖRL, E. M., BROWN, H. W. & BROIDA, H. P. (1959). *J. Chem. Phys.* **30**, 1304.

RUHEMANN, M. (1932). *Z. Phys.* **76**, 368.

SCHMID, E. & BOAS, W. (1935). *Kristallplastizität*, Berlin.

VEGARD, L. (1929). *Z. Phys.* **58**, 297.

WILSON, A. J. C. (1942). *Proc. Roy. Soc.* A, **180**, 277.

Acta Cryst. (1961). **14**, 19

Magnetic Structures of 3*d* Transition Metal Double Fluorides, K*Me*F$_3$*

BY VLADIMIRO SCATTURIN,† LESTER CORLISS, NORMAN ELLIOTT AND JULIUS HASTINGS

Department of Chemistry, Brookhaven National Laboratory, Upton, Long Island, New York, U.S.A.

(*Received* 23 *October* 1959 *and in revised form* 6 *February* 1960)

The antiferromagnetic structures of $KCrF_3$, $KMnF_3$, $KFeF_3$, $KCoF_3$, $KNiF_3$, and $KCuF_3$, have been obtained by neutron diffraction. The Mn, Fe, Co, and Ni double fluorides exhibit an ordering in which the divalent 3*d* ion is coupled antiferromagnetically to its six nearest neighbors. In the chromium double fluoride, the magnetic structure consists of ferromagnetic (001) sheets, coupled antiferromagnetically along the [001] direction. No magnetic scattering is observed in the neutron diffraction pattern of the copper double fluoride.

The magnetic structures and the observed crystallographic distortions are discussed in terms of an indirect exchange mechanism and in terms of the crystal field theory, respectively.

Introduction

Ionic compounds of formula ABX_3 often crystallize in the perovskite structure, provided the A and X ions form close-packed AX_3 layers and the B ion can be accommodated in the holes between these layers. When magnetically active B ions are introduced into this structure, there is a possibility of interaction leading to magnetic ordering. Antiferromagnetic structures have, indeed, been observed in perovskite-like double oxides of 3*d* trivalent ions: the so-called A-type configuration was observed for Mn^{+3} in $LaMnO_3$ (Wollan & Koehler, 1955) while the G-type was found for Mn^{+4} in $CaMnO_3$ (Wollan & Koehler, 1955), for Fe^{+3} and Cr^{+3} in $LaFeO_3$ and $LaCrO_3$ (Koehler & Wollan, 1957). Similar magnetic configurations were observed in the trifluorides of 3*d* transition metals (Wollan, Child, Koehler & Wilkinson, 1958), which have a crystal structure related to the perovskite structures. Indirect exchange interactions, depending on the electronic configuration of the ions and the crystal structure, presumably account for the magnetic ordering of these compounds. As in all indirect exchange couplings the anions play an important rôle in the exchange interaction.

A neutron diffraction study has been made of the magnetic structures of 3*d* metal double fluorides, K*Me*F$_3$, containing divalent magnetic ions and having a perovskite-like structure. The main purposes of this study were to find the magnetic ordering of the metal ions and to correlate the spin arrangement with the properties of the orbitals involved in the indirect exchange.

3*d* divalent ions and crystal field theory

It is convenient, for the subsequent discussion, to review at this point the properties of 3*d* divalent ions

* Research performed under the auspices of the U.S. Atomic Energy Commission.

† Present address: Istituto di Chimica Generale e Inorganica, Universita di Padova, Padova (Italy).